

Resonant tunneling in a schematic model

Sonia Bacca* and Hans Feldmeier†

Gesellschaft für Schwerionenforschung, Planckstr. 1, D-64291 Darmstadt, Germany

(Received 24 February 2006; published 19 May 2006)

Tunneling of a harmonically bound two-body system through an external Gaussian barrier is studied in a schematic model that allows for a better understanding of intricate quantum phenomena. The role of finite size and internal structure is investigated in a consistent treatment. The excitation of internal degrees of freedom gives rise to a peaked structure in the penetration factor. The model results indicate that for soft systems the adiabatic limit is not necessarily reached, although often assumed in the fusion of nuclei and in electron screening effects at astrophysical energies.

DOI: [10.1103/PhysRevC.73.054608](https://doi.org/10.1103/PhysRevC.73.054608)

PACS number(s): 24.10.Eq, 03.65.Xp, 25.60.Pj, 25.70.Ef

I. INTRODUCTION

The phenomenon of quantum tunneling is relevant in several areas of physics, from chemical reactions and electronic circuits to nuclear fission and fusion processes below the Coulomb barrier. In many cases, one has to deal with the tunneling of composite objects. In general, one tries to identify macroscopic degrees of freedom (denoted by R) and intrinsic ones (denoted by ξ), decomposing the Hamiltonian accordingly,

$$H = H_{\text{mac}}(R) + H_{\text{int}}(\xi) + V(R, \xi). \quad (1)$$

The macroscopic part, $H_{\text{mac}}(R)$, is the Hamiltonian for the (few) collective variables and contains not only the collective kinetic energy but also the macroscopic potential that has to be transversed by quantum tunneling. $H_{\text{int}}(\xi)$ contains the (many) intrinsic degrees of freedom of the many-body system, while $V(R, \xi)$ describes an interaction between intrinsic and macroscopic variables. For example, if one wants to describe electron screening effects at astrophysical energies [1], R could be the distance between the nuclei of two fusing atoms and ξ could denote the electron degrees of freedom. Or in nuclear physics, R may denote the shape degrees of freedom for a heavy nucleus that undergoes spontaneous fission and ξ the individual nucleon degrees of freedom (see, for example [2]). The question of how the tunneling reaction is influenced by finite size and structure of the composite object is an intriguing one. An important aspect is to determine which degree of freedom must be taken into account in a theoretical description and which can be neglected. The description of the tunneling of a composite object with many degrees of freedom is a very complex many-body problem. Therefore, very often radical approximations are made. As an example, nuclear cross sections at very low energy, which are important in astrophysics and for which no experimental data exist, are often determined by extrapolations based on the one-dimensional result for pointlike particle tunneling. On the other hand, in heavy-ion fusion reactions, it is well known that the coupling of the relative motion of the colliding nuclei with the nuclear intrinsic motion strongly enhances the fusion cross

section in the subbarrier energy region. This was proven in a number of precise experiments, where the fusion cross section for intermediate mass systems (see, e.g. [3]) was found to be higher than a simple one-dimensional prediction for tunneling through a potential barrier formed by the attractive nuclear interaction and the repulsive Coulomb force. The coupling between macroscopic and microscopic coordinates has been studied in multidimensional approaches (with many internal degrees of freedom), with different coupling schemes and with different approximations (see Ref. [4] and references therein).

In this paper, we investigate the relation between the translational motion and the internal degrees of freedom of a composite object in a schematic but fully consistent model. In spite of the simplicity of the model, it has all the ingredients needed to understand, for example, the subbarrier fusion of soft nuclei, which can easily vibrate. In fact, the low energy fusion cross section is usually dominated by s -wave fusion so that one deals only with one collective variable, the radial coordinate R , and a few low-lying excited states [4], as in the schematic model we describe in the following.

II. THE MODEL

The Hamiltonian of two interacting particles with identical mass m under the influence of an external potential barrier is

$$H(x_1, x_2) = -\frac{\hbar^2}{2m} \left[\frac{d^2}{dx_1^2} + \frac{d^2}{dx_2^2} \right] + V_{\text{int}}(x_1 - x_2) + V(x_1) + V(x_2), \quad (2)$$

where $x_{1,2}$ denote the coordinates of particles 1 and 2, respectively, while V_{int} and V are the intrinsic potential and external barrier, felt by both particles. Performing a transformation to the center of mass (c.m.) and relative coordinate denoted by R and ξ , respectively, the Hamiltonian becomes

$$H(R, \xi) = -\frac{\hbar^2}{2M} \frac{d^2}{dR^2} + H_{\text{int}}(\xi) + V \left(R + \frac{\xi}{2} \right) + V \left(R - \frac{\xi}{2} \right). \quad (3)$$

Here $H_{\text{int}}(\xi) = -\frac{\hbar^2}{2\mu} \frac{d^2}{d\xi^2} + V_{\text{int}}(\xi)$ is the Hamiltonian of the intrinsic system, while $M = 2m$ and $\mu = m/2$ represent the center of mass and the reduced mass, respectively. As one can

*Electronic address: s.bacca@gsi.de†Electronic address: h.feldmeier@gsi.de

see, the external potential, depending on its functional form, may generate coupling terms of different orders between the macroscopic and the internal coordinates.

The standard theoretical approach to studying the effect of internal excitations induced by the coupling potential is to solve the coupled-channel equations, which in our case read

$$-\frac{\hbar^2}{2M} \frac{d^2}{dR^2} \phi_{ji}(R) + \sum_{n=0}^N [V_{jn}(R) + (\epsilon_n - E) \delta_{jn}] \phi_{ni}(R) = 0, \quad (4)$$

where E is the total energy of the system and ϵ_n is the internal excitation energy. These equations are obtained by introducing the eigenstates of the internal systems, i.e.,

$$\left(-\frac{\hbar^2}{2\mu} \frac{d^2}{d\xi^2} + V_{\text{int}}(\xi) \right) \chi_n(\xi) = \epsilon_n \chi_n(\xi), \quad (5)$$

and expanding the total wave function as

$$\varphi(R, \xi) = \sum_{n=0}^N \phi_{ni}(R) \chi_n(\xi), \quad (6)$$

N being the number of internal excitations considered. The expansion coefficients $\phi_{ni}(R)$ depend on the c.m. coordinate. Here the subindex i denotes the initial channel, i.e., the starting energy level of the internal system. In Eq. (4), the potential matrix elements

$$V_{jn}(R) = \int_{-\infty}^{\infty} d\xi \chi_j^*(\xi) \left[V \left(R + \frac{\xi}{2} \right) + V \left(R - \frac{\xi}{2} \right) \right] \chi_n(\xi) \quad (7)$$

can be interpreted as the effective potentials felt by the c.m. due to the presence of internal degrees of freedom.

Equation (4) consists of a set of N coupled second-order differential equations, and in case the particle is incident on the barrier from the left-hand side, the boundary conditions we require for its solution are

$$\begin{aligned} \lim_{R \rightarrow -\infty} \phi_{ni}(R) &= \delta_{ni} e^{ik_n R} + A_{ni} e^{-ik_n R}, \\ \lim_{R \rightarrow \infty} \phi_{ni}(R) &= B_{ni} e^{ik_n R}. \end{aligned} \quad (8)$$

Here $k_n = \sqrt{2M(E - \epsilon_n)/\hbar^2}$ is the wave number of the n -th channel. The inclusive penetration factor, or total transmission coefficient, is then given by

$$T = \sum_{n=0}^N T_{ni}, \quad (9)$$

where the transmission probability for each channel is defined as

$$T_{ni} = \frac{k_n}{k_i} |B_{ni}|^2. \quad (10)$$

In the schematic model that we would like to solve, we assume a harmonic internal potential $V_{\text{int}}(\xi) = \frac{1}{2} \mu \Omega^2 \xi^2 - \frac{1}{2} \hbar \Omega$ and a Gaussian external barrier $V(x) = V_0 e^{-v^2 x^2}$. In this case, the internal excitation energy becomes $\epsilon_n = n \hbar \Omega$ and the effective potential matrix elements have the analytical

form [5,6]

$$\begin{aligned} V_{jn}(R) &= 4V_0 \frac{\beta}{(2^{j+n} n! j!)^{1/2}} \frac{e^{-\frac{4\beta^2 v^2 R^2}{4\beta^2 + v^2}}}{(4\beta^2 + v^2)^{1/2}} \\ &\times \sum_{k=0}^{\min(n,j)} 2^k k! \binom{j}{k} \binom{n}{k} \left(\frac{v^2}{4\beta^2 + v^2} \right)^{\frac{j+n}{2} - k} \\ &\times H_{j+n-2k} \left(-\frac{2v\beta R}{(4\beta^2 + v^2)^{1/2}} \right), \end{aligned} \quad (11)$$

if $n + j$ is even; and $V_{jn}(R) = 0$ otherwise, where $\beta = (\mu \Omega / \hbar)^{1/2}$ is the harmonic oscillator parameter. We would like to emphasize that in this case, the potential matrix elements can be calculated exactly and treated consistently within the model: they are given by the product of a Gaussian function and a linear combination of Hermite polynomials. Therefore, they may show some structure depending on the chosen parameters. This is not equivalent to making a separable ansatz for the coupling potential and then assuming constant form factors or a Gaussian parametrization as proposed in Ref. [7]. One can note that the potential matrix elements of (11) connecting channel j with channel n depend on the internal system via the β parameter. The first matrix element, V_{00} , which accounts for the elastic transition from the ground state ($j = 0$) to itself ($n = 0$), is a simple Gaussian function whose width depends on the original width of the external barrier ($\sim 1/v$) and on the harmonic oscillator parameter β . In case of a very stiff internal harmonic oscillator, i.e., for $\Omega \rightarrow \infty$, one sees that $V_{00}(R) \rightarrow 2V(R)$. This is the limit case in which the composite object behaves like a point particle, feeling two times the external potential. Thus, for finite Ω the diagonal matrix elements V_{nn} account for the finite-size effect, while the coupling terms ($n \neq j$) are responsible for transition to the excited states. Performing a Taylor expansion of the coupling potential for $\xi \ll 1/v$ up to the second order one gets

$$V \left(R + \frac{\xi}{2} \right) + V \left(R - \frac{\xi}{2} \right) = 2V(R) + V''(R) \frac{\xi^2}{4} + \dots \quad (12)$$

In case the two-body system is composed of identical particles, both interacting with a symmetrical external barrier, the coupling potential does not include any linear coupling term as $V'(R)\xi$. Actually, it consists of an expansion over all even coupling terms. This means that the barrier effect on the intrinsic system is reduced, up to the second order of the expansion, to an additional harmonic potential that shrinks or stretches it, depending on whether the second derivative of the external potential is positive or negative, respectively. By comparing the intrinsic harmonic potential V_{int} with the induced harmonic potential $V''(R) \frac{\xi^2}{4}$, for example, at $R = 0$ where $V''(R)$ presents a minimum with maximal amplitude, one can say that if $\hbar \Omega > \hbar v \sqrt{V_0/\mu}$ (or $\hbar \Omega < \hbar v \sqrt{V_0/\mu}$) the intrinsic system is stiff (or soft) with respect to induced excitations. If the object is very stiff, one expects the internal excitation to play a negligible role; whereas in case of a very soft system, many internal levels have to be taken into account.

In the following, we solve the coupled channel problem using the potential matrix elements of Eq. (11). In order to gain

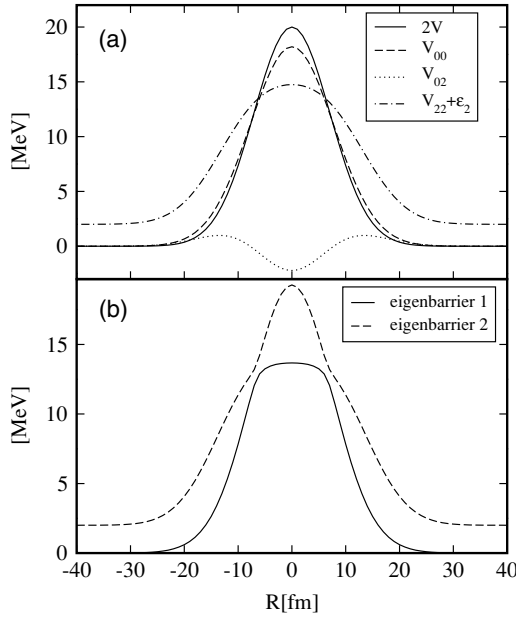


FIG. 1. Effective potential matrix elements for a two-level system in comparison with the external barrier (parameters are $\hbar\Omega = 1$ MeV, $m = 938$ MeV, $V_0 = 10$ MeV, and $\nu = 0.1$ fm⁻¹).

insight into the effect of the coupling, we restrict ourselves to the case of a two-level system. The internal degrees of freedom are taken to be initially in the ground state with excitation energy ϵ_0 . Thus, in the presented model the only possible transition will be to the second excited state ($n = 2$), since the coupling term $V_{01}(R)$ vanishes because of the mirror symmetry of the Gaussian barrier. For our two-level system, we can then define the potential matrix as

$$W(R) = \begin{pmatrix} V_{00}(R) & V_{02}(R) \\ V_{20}(R) & V_{22}(R) + \epsilon_2 \end{pmatrix}, \quad (13)$$

where $\epsilon_2 = 2\hbar\Omega$ is the energy difference between the two levels, being $\epsilon_0 = 0$. Since we are interested in studying the effect of induced internal excitations, we will start to consider a soft object, for which the internal structure plays a relevant role. In our first analysis, we use the following parameters: harmonic oscillator frequency $\hbar\Omega = 1$ MeV, mass $m = 938$ MeV, barrier amplitude $V_0 = 10$ MeV, barrier inverse width $\nu = 0.1$ fm⁻¹, which lead to $\hbar\nu\sqrt{V_0/\mu} = 2.88$ MeV.

In Fig. 1(a), we first show the consistent potential matrix elements of Eq. (11) for the chosen parameters, in comparison with the external barrier. One can note that due to the finite size effect, the potentials V_{00} and V_{22} show a broadened structure with respect to the external potential, while the coupling term V_{02} changes sign two times. In Fig. 1(b), we present the so-called eigenbarriers (or eigenpotentials), obtained by diagonalizing the potential matrix of Eq. (13) at each position of the macroscopic coordinate R (see, e.g. [8]).

We have then performed the coupled channel calculation, integrating Eq. (4) from $R = -40$ fm to $R = 40$ fm and imposing the incoming wave boundary condition of Eq. (8). It is known that with this method, often used in heavy-ion collision calculations [9], it is sometimes difficult to obtain

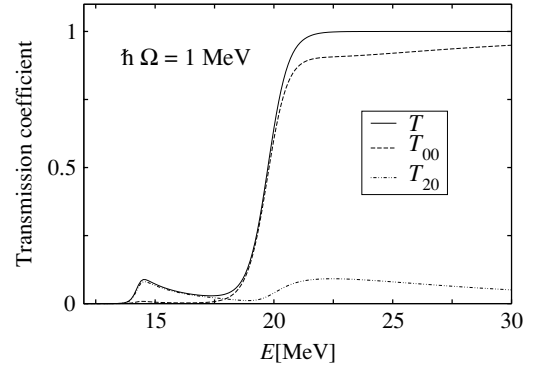


FIG. 2. Total transmission coefficient and separate T_{20} and T_{00} contributions as functions of the total energy of the system for $\hbar\Omega = 1$ MeV.

a stable solution with a controlled numerical accuracy. In order to check the numerical results, we also solve the problem with the more stable method of the variable reflection amplitude [5], with which the set of two coupled second-order linear differential equations is transformed into a set of four coupled nonlinear first-order differential equations. Other similar methods have been proposed to stabilize the numerical solutions of the coupled channel problem (see, e.g. [10]). We obtained the same result with the above mentioned two methods with a relative percentage error of about 1%–3% in the presented energy region, indicating that the numerical accuracy is under control in the considered example.

In Fig. 2, we show the result of the total transmission coefficient T and of separate contributions T_{20} and T_{00} . As one can see, the penetration factor presents a peaked structure at a total energy value of about $E_{\text{peak}} = 14$ MeV. The pronounced peak is mainly due to excitation to the energy level ϵ_2 , as can be seen from the fact that T_{20} also presents a peak, while the elastic channel T_{00} is rather flat in this energy region. This agrees with the intuitive picture that the system avoids the higher barrier V_{00} by going to the excited state which then tunnels easily through the lower barrier $V_{22} + \epsilon_2$ (see Fig. 1). However, this picture does not hold for higher energies where the situation is inverted because of the effect of the coupling; and finally, for energies somewhat higher than the external barrier (20 MeV), the elastic channel T_{00} dominates the total transmission. Thus, a proper treatment of the coupling V_{02} is important.

We would like to point out that the consistent treatment of the internal degrees of freedom in Eq. (7) produces different widths for the diagonal potential matrix elements and oscillations in the coupling term. This leads to the emergence of a resonant structure in the penetration factor. A peak in the transmission coefficient is not found if one parametrizes each potential matrix element with a simple Gaussian function with the same width as done in [7,8,11], where a shoulderlike structure is found.

We can then investigate the effect of the different stiffnesses of the composite object by keeping the same parameters for the external barrier and changing the internal frequency of the harmonic oscillator. In Fig. 3, we show the transmission coefficients for different values of $\hbar\Omega$ as a function of the

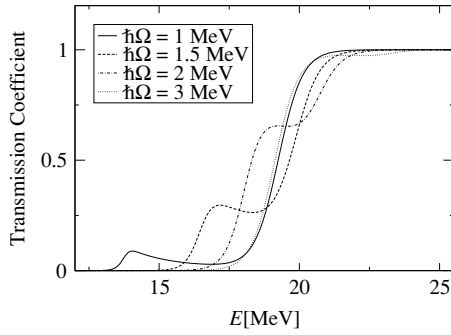


FIG. 3. Transmission coefficients for different values of the harmonic oscillator frequency as a function of total energy.

total energy. One can see that the peaked structure moves toward higher energies with growing intrinsic frequency. When $\hbar\Omega$ is larger than $\hbar\nu\sqrt{V_0/\mu}$, the structure in T becomes less pronounced and more similar to a shoulder, as found in [8]. The reason is that as Ω increases, the widths of the diagonal matrix elements V_{00} and V_{22} become more similar and the coupling V_{02} gets smaller, leading to a potential matrix similar to the parametrization of Ref. [8] for high excitation energies. For $\hbar\Omega = 2$ MeV and higher, the transmission coefficient at low energy is dominated by the elastic channel T_{00} , since the consistent treatment of the potential matrix elements gives a V_{00} barrier lower than that of $V_{22} + \epsilon_2$, in contradistinction to the case of $\hbar\Omega = 1$ MeV depicted in Fig. 1.

We also investigated the model with two excited intrinsic states. In general, the three-level system picture within this consistent model leads to the emergence of two peaked structures: the position of the first peak is shifted toward lower energies and that of the second toward higher energies with respect to the location of the single peak found in the two level system. Such a behavior was also found for the shoulderlike structure of the three-level system in [11] with respect the two-level system in [8]. In the case of three levels, the structure of the consistent matrix elements becomes more complicated; therefore, we prefer to stick to the simpler two-level approach to further understand the effect of the coupling.

In order to estimate the dynamic effect due to excitation of internal degrees of freedom, one should compare the coupled channel calculation with the uncoupled problem, where only the potential V_{00} is considered. As already mentioned, this matrix element does not allow for internal transitions, but it still accounts for finite size effects. This is different from tunneling through the bare barrier $2V$, since this would be equivalent to reducing the problem to the tunneling of a pointlike particle. In Fig. 4, we show the above mentioned transmission coefficients in the case of a soft object, i.e., for $\hbar\Omega = 1$ MeV. In the peak region, the effect of the excitation of the internal degrees of freedom leads to an enhancement of the transmission coefficient T of about five orders of magnitude. On the other hand, at higher energies the tunneling probability is lower than in the case of no coupling. The enhancement of T in the coupled channel calculation with respect to the no coupling case strongly depends on the harmonic oscillator frequency: it decreases with growing Ω , i.e., with increasing stiffness of the composite object. In Fig. 4, we also compare our result

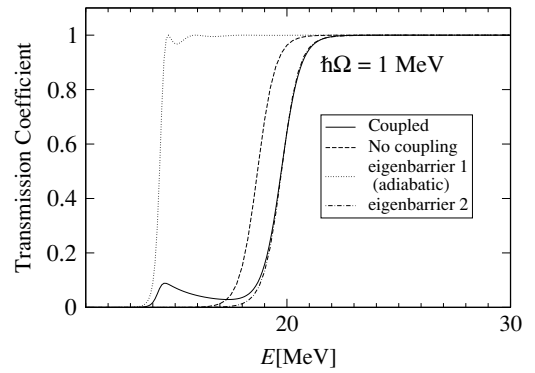


FIG. 4. Effects of the internal degrees of freedom for $\hbar\Omega = 1$ MeV: comparison of the coupled channel result with the no coupling calculation. Transmission coefficients for tunneling through the eigenbarriers are also shown.

with the transmission coefficients found for tunneling through the eigenbarriers of the two-level system. In the following we recall the meaning of the eigenbarriers.

Considering the part of the Hamiltonian of Eq. (3) that depends on the intrinsic coordinate, i.e.,

$$\tilde{H}(R, \xi) = H_{\text{int}}(\xi) + V\left(R + \frac{\xi}{2}\right) + V\left(R - \frac{\xi}{2}\right), \quad (14)$$

one can define the adiabatic states by minimizing it with respect to the internal degrees of freedom at each position R [4]. This translates then into an eigenvalue problem, which in our case reads

$$W(R) \begin{pmatrix} \phi_0(R) \\ \phi_2(R) \end{pmatrix} = \lambda \begin{pmatrix} \phi_0(R) \\ \phi_2(R) \end{pmatrix}, \quad (15)$$

with $W(R)$ as defined in Eq. (13). The solution of the eigenvalue problem is found by diagonalizing the potential matrix, i.e., by considering the eigenbarriers. In the literature, tunneling through the lowest eigenbarrier is often called adiabatic transition.

As one can notice from Fig. 4, the adiabatic picture is very different from the result of the coupled channel calculation, though a small structure is found in adiabatic tunneling in the same position as the pronounced peak of the coupled calculation. Furthermore, we observe that the adiabatic transmission coefficient is always larger than the coupled result. For higher energy, the coupled channel calculation agrees with the result obtained for tunneling through the second eigenbarrier.

The concept of eigenbarriers is useful in case one wants to describe the fusion cross section as given by an average over the contribution from each eigenbarrier with appropriate weight factors. A method to extract the barrier distribution from the measured cross section was proposed in Ref. [12]. From a purely theoretical point of view, the barrier distribution picture is correct only when the transformation that diagonalizes the matrix $W(R)$ does not depend on the coordinate R . An approximation which is often made consists in considering the eigenbarriers and then evaluating the weight factor at a fixed position of R , assuming them to be constant. In Ref. [8], it was shown that in the case where one parametrizes the potential matrix elements by Gaussians of the same width, the

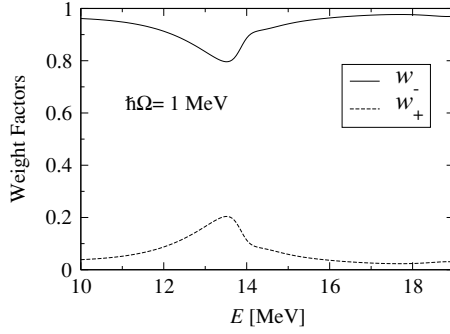


FIG. 5. Weight factors for two eigenbarriers in the case of $\hbar\Omega = 1$ MeV.

weight factors are almost constant as a function of energy. It was also proven that they are very different from those approximately estimated at the location of the maximum of the bare barrier [13]. For a two-level system, the weight factors are given by [8]

$$\begin{aligned} w_-(E) &= [T(E) - T_-(E)] / [T_+(E) - T_-(E)], \\ w_+(E) &= [T_+(E) - T(E)] / [T_+(E) - T_-(E)], \end{aligned} \quad (16)$$

where $T_{-,+}(E)$ denote the transmission coefficients for the first and second eigenbarrier, respectively, and $T(E)$ is the total transmission as calculated in the coupled channel case. In Fig. 5, we show these optimum weight factors in our consistent model for the case of $\hbar\Omega = 1$ MeV. One can note that they are not constant in the energy region where the peaked structure in T is presented, showing that the approximation of constant weight factors does not hold. This is related to the fact that the transition is not adiabatic, as already discussed. We observe that with increasing stiffness of the composite object, the weight factor shows a less pronounced variation as a function of the energy.

In order to gain more insight into the meaning of the adiabatic picture, we recall that in the case of a two-level system, the orthogonal rotation that is needed to diagonalize the symmetric matrix $W(R)$ can be parametrized by one single mixing angle $\theta(R)$ as

$$\mathcal{R}_{\theta(R)} = \begin{pmatrix} \cos \theta(R) & \sin \theta(R) \\ -\sin \theta(R) & \cos \theta(R) \end{pmatrix}. \quad (17)$$

At this point, if one would like to transform the coupled channel equation of (4), one should accordingly also transform the kinetic energy, which does not commute with the rotation operator, which depends on the coordinate R . In fact, denoting the diagonal kinetic energy matrix as K , the transformed matrix looks like

$$\begin{aligned} &\mathcal{R}_{\theta(R)}^T K \mathcal{R}_{\theta(R)} \\ &= \frac{\hbar^2}{2M} \begin{pmatrix} -\frac{d^2}{dR^2} + (\theta'(R))^2 & -\theta''(R) - 2\theta'(R)\frac{d}{dR} \\ \theta''(R) + 2\theta'(R)\frac{d}{dR} & -\frac{d^2}{dR^2} + (\theta'(R))^2 \end{pmatrix}. \end{aligned} \quad (18)$$

Thus, one can see that the adiabatic picture, which consists in considering only the first eigenbarrier solving an uncoupled problem, is valid when the first and second derivative of the

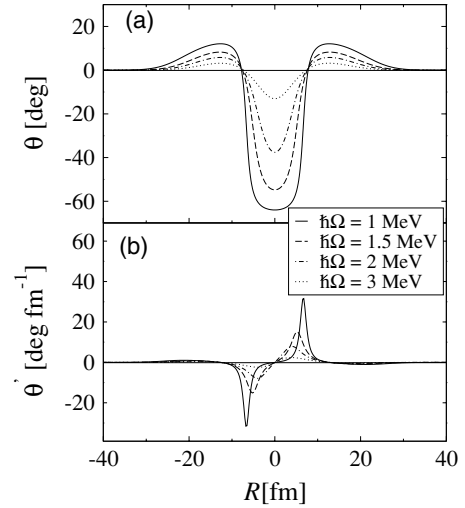


FIG. 6. Mixing angle and its first derivative as a function of c.m. coordinate for different values of $\hbar\Omega$.

mixing angle are negligible, i.e., when the transformed kinetic energy tends to the original diagonal one. In order to see whether this is the case in the considered example, we show in Fig. 6 the mixing angle (a) and its derivative (b) for different values of the internal frequency Ω as a function of the c.m. coordinate. First, one notes that in all cases θ crosses zero two times; these are the two points in which the coupling matrix element $V_{02}(R) = 0$ and thus $W(R)$ is already diagonal. This is not the case if one parametrizes all matrix elements with Gaussian functions of the same width as was done in [7,8], where the mixing angle is always positive and can be a maximal 45° in the case of strong coupling. If one then focuses on the softer case of $\hbar\Omega = 1$ MeV, which corresponds to the example shown in Figs. 2 and 4, one observes that the angle suddenly changes sign, going from about 12° to about -64° . The derivative of the mixing angle is thus very large in the vicinity of the two zeros of θ . For this reason, its contribution in the transformed kinetic energy is not negligible. In fact, the extra diagonal term $\frac{\hbar^2}{2M}(\theta'_{\max})^2$, which is about 3.25 MeV at $R = \pm 6.6$ fm, has to be added to the adiabatic potential, which is maximally 13.67 MeV. Moreover, the off-diagonal matrix elements contain the second derivative of $\theta(R)$ which gives maximum values of $\frac{\hbar^2}{2M}\theta''_{\max} \approx 4.34$ MeV, thereby invalidating the adiabatic assumption.

The rapid change of the mixing angle is related to a so-called Landau-Zener pseudocrossing of the two levels [14]. Denoting the rotated state with

$$\begin{pmatrix} \tilde{\phi}_0(R) \\ \tilde{\phi}_2(R) \end{pmatrix} = \mathcal{R}_{\theta(R)} \begin{pmatrix} \phi_0 \\ \phi_2 \end{pmatrix} \quad (19)$$

and considering the optimal case in which the mixing angle varies suddenly as $\theta(R_1) \rightarrow \theta(R_2) = \theta(R_1) \pm \pi/2$ going from coordinate R_1 to R_2 , one can note that the two rotated states invert each other in the sense $\tilde{\phi}_0(R_1) \rightarrow \tilde{\phi}_2(R_2)$ and $\tilde{\phi}_2(R_1) \rightarrow \tilde{\phi}_0(R_2)$. In other words, the first energy level suddenly becomes the second and vice versa. In case of a soft object, the variation of the mixing angle does not give rise to the maximal

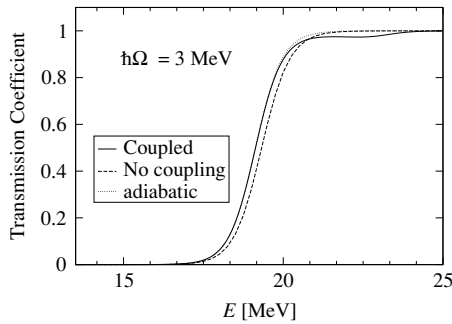


FIG. 7. Comparison of the coupled channel result with the no coupling calculation and with the adiabatic transition for $\hbar\Omega = 3$ MeV.

pseudocrossing; but still, for example, at $R_1 \approx -14$ fm, we have $\theta = 12^\circ$ and $\tilde{\phi}_0(R_1) = (0.98\phi_0 + 0.21\phi_2)$, and at $R_2 = 0$, we have $\theta = -64^\circ$ with $\tilde{\phi}_2(R_2) = (0.90\phi_0 + 0.44\phi_2)$, so that $\tilde{\phi}_2(R_1)$ and $\tilde{\phi}_2(R_2)$ are very similar. Therefore, there is partial pseudocrossing which is related to a nonadiabatic transition, as discussed above. In fact, looking at Fig. 6 one can see that if the composite object becomes stiffer, then the mixing angle is smaller and does not vary so rapidly as a function of the c.m. coordinate; i.e., there is no Landau-Zener crossing any more. For this reason, one expects the adiabatic limit to be recovered for a stiff object. To illustrate that, we show in Fig. 7 the transmission coefficient obtained from the coupled channel calculation, the no coupling case, and the adiabatic one for $\hbar\Omega = 3$ MeV. One can note that for energies lower than the external barrier, the adiabatic limit is now recovered (dotted curve lies on top of the solid line). This time, $\frac{\hbar^2}{2M}(\theta'_{\max})^2 \approx 0.018$ MeV and $\frac{\hbar^2}{2M}\theta''_{\max} \approx 0.19$ MeV, and thus the changes in the kinetic energy matrix (18) are negligible. The coupling to the excited state still leads to a higher penetration factor with respect to the uncoupled case. For even stiffer systems, for example, $\hbar\Omega = 5$ MeV, we observe that the coupled calculation finally coincides also with the uncoupled and the adiabatic one. We do not obtain

an energy shift of the coupled result with respect to the uncoupled case as in [8], since in our consistent treatment, the excitation energy and the potential matrix element are not independent from each other: with growing Ω , the excitation energy increases, but the coupling potential $V_{02}(R)$ goes to zero. When the object is too stiff to be excited, no structure is found in the transmission coefficient: the internal system starts from the ground state and emerges still in the ground state at the end of the barrier. In this limiting case, a coupled channel calculation is not necessary, since the internal degrees of freedom do not play any role.

III. SUMMARY AND CONCLUSIONS

To summarize, we present a schematic model to describe the tunnel effect of a two-body system in a two-level approximation. Assuming a harmonic oscillator as the internal interaction and a Gaussian external barrier, one can give a consistent description of the potential felt by the macroscopic coordinate due to the presence of internal degrees of freedom. No *a priori* parametrization of the potential matrix elements is assumed. Therefore, in the coupled channel picture, the dynamics of the internal degrees of freedom and their interaction with the external barrier are treated consistently. Not only does a stiffer system have a larger intrinsic excitation energy but also the potential matrix elements change accordingly. The coupled channel calculation shows a peaked structure in the transmission coefficient that accounts for the excitation of the intrinsic system. We show that for a soft object the mixing angle is large and rapidly changes sign, so the adiabatic limit is not approached at low energies. The resonant transition to the excited state is explained by a Landau-Zener level crossing in a nonadiabatic picture. As expected, the adiabatic limit is recovered in the case of a stiff object, where the energy is not sufficient to excite the internal structure. The model results suggest that one should investigate more carefully the fusion of soft nuclei or electron screening at astrophysical energies, where the adiabatic approximation often is used.

-
- [1] K. Langanke, in *Advances in Nuclear Physics*, edited by J. W. Negele and E. Vogt (Plenum Press, New York, 1994), Vol. 21, p. 85.
 - [2] H. Goutte, J. F. Berger, P. Casoli, and D. Gogny, *Phys. Rev. C* **71**, 024316 (2005).
 - [3] A. M. Stefanini *et al.*, *Phys. Rev. Lett.* **74**, 864 (1995).
 - [4] A. B. Balantekin and N. Takigawa, *Rev. Mod. Phys.* **70**, 77 (1998).
 - [5] M. Razavy, *Quantum Theory of Tunneling* (World Scientific, Singapore, 2003).
 - [6] I. S. Gradshteyn and I. M. Ryzhik, *Table of Integrals, Series and Products* (Academic Press, New York, 1965).
 - [7] C. H. Dasso, S. Landowne, and A. Winther, *Nucl. Phys.* **A405**, 381 (1983); **A407**, 221 (1983).
 - [8] K. Hagino, N. Takigawa, and A. B. Balantekin, *Phys. Rev. C* **56**, 2104 (1997).
 - [9] S. Landowne and S. C. Pieper, *Phys. Rev. C* **29**, 1352 (1984).
 - [10] W. Brenig, T. Brunner, A. Gross, and R. Russ, *Z. Phys. B* **93**, 91 (1993).
 - [11] K. Hagino and A. B. Balantekin, *Phys. Rev. A* **70**, 032106 (2004).
 - [12] R. G. Rowley, G. R. Satchler, and P. H. Stelson, *Phys. Lett.* **B254**, 25 (1991).
 - [13] C. H. Dasso and S. Landowne, *Phys. Lett.* **B183**, 141 (1987).
 - [14] L. D. Landau, *Phys. Z. Sowjetunion* **2**, 46 (1932); G. Zener, *Proc. R. Soc. London Ser. A* **137**, 696 (1932); L. D. Landau and E. M. Lifshitz, *Quantum Mechanics: Non Relativistic Theory* (Pergamon, New York, 1977), Vol. 3.